



Environmental pH is a key modulator of *Staphylococcus aureus* biofilm development under predation by the virulent phage phiIPLA-RODI

Lucía Fernández^{1,2}  · Diana Gutiérrez^{1,3} · Pilar García^{1,2} · Ana Rodríguez^{1,2}

Received: 15 April 2020 / Revised: 3 September 2020 / Accepted: 14 September 2020 / Published online: 22 September 2020
© The Author(s), under exclusive licence to International Society for Microbial Ecology 2020

Abstract

Previous work had shown that, in some *Staphylococcus aureus* strains, low concentrations of the virulent phage vB_SauM_phiIPLA-RODI (phiIPLA-RODI) promoted the formation of DNA-rich biofilms, whose cells exhibited significant transcriptional differences compared to an uninfected control. This study aimed to dissect the sequence of events leading to these changes. Analysis of phage propagation throughout biofilm development revealed that the number of phage particles increased steadily up to a certain point and then declined. This partial phage inactivation seemed to be a consequence of medium acidification due to glucose fermentation by the bacterium. Computer simulation of phage–host dynamics during biofilm development showed how even small differences in pH evolution can affect the outcome of phage infection. An acidic pH, together with successful phage propagation, was also necessary to observe the phage-associated changes in biofilm architecture and in the transcriptional profile of the bacterial population. Altogether, this study shows how the dynamics between phage and host can be tightly coordinated through an environmental cue, even in the context of a complex biofilm population.

Introduction

As highly specialized predators, bacteriophages need to coexist with their bacterial hosts. Indeed, prey extinction would unavoidably lead to disappearance of the viral population. Temperate phages avoid this by integrating into the host chromosome at a frequency that depends on the environmental conditions [1]. It is not so clear, however, how virulent phages, i.e., those that only follow the lytic

cycle, achieve coexistence. Some authors have explored “Red Queen” models of a co-evolutionary arms race [2], or fluctuating selection dynamics (FSD) [3], two strategies that may alternate depending on the environmental conditions [4, 5]. In the first model, phage infectivity and bacterial resistance increase over time up to a certain point, while FSD reflects the existence of a fluctuation in the resistance and infectivity phenotypes. In some environments, however, the phenomenon of local adaptation seems indicative of a higher selective pressure on the phage population to become more infective than on the bacterial population to acquire resistance [6]. Another explanation of phage–host coexistence would be the likelier selection of phages that are “mediocre killers” compared to more efficient phage variants that would rapidly die off after eradicating their host [7]. This reduced virulence may be achieved through the evolution of various phage life traits (e.g., reduced adsorption, delayed lysis, etc.). Another potential factor is spatial heterogeneity, as is observed in soil and biofilms, which might slow down phage propagation and favor the evolution of more “cautious” infection strategies (e.g., mediocre killers, vertical transmission, etc.), as well as favor low interaction rates between phage and bacteria [8]. A recent study has found that spatial heterogeneity also plays

Supplementary information The online version of this article (<https://doi.org/10.1038/s41396-020-00778-w>) contains supplementary material, which is available to authorized users.

✉ Lucía Fernández
lucia.fernandez@ipla.csic.es

¹ Instituto de Productos Lácteos de Asturias (IPLA-CSIC), Paseo Río Linares s/n, 33300 Villaviciosa, Asturias, Spain

² DairySafe Group, Instituto de Investigación Sanitaria del Principado de Asturias (ISPA), Oviedo, Spain

³ Present address: Laboratory of Applied Biotechnology, Department of Applied Biosciences, Faculty of Bioscience engineering, Ghent University, 9000 Ghent, Belgium

a role in bacterial communities living in the mammalian gut [9]. A further possibility for coexistence is related to the phenomenon of phenotypic resistance [10, 11]. Nonetheless, there may be additional factors influencing the balance between phage propagation and decay that may ultimately lead to co-survival, perhaps in coordination with bacterial growth. For instance, propagation rates vary according to the metabolic state of the host, which is, in turn, dependent on nutrient availability [12, 13]. Additionally, production of certain bacterial metabolites at certain growth stages might, as a collateral effect, contribute to phage inactivation if they have a deleterious impact on phage particle stability [14]. Understanding the nature of such interactions would help us acquire a more realistic view of phage–host dynamics, and might provide some clues regarding the potential effect of releasing bacteriophages into the environment for therapeutic purposes.

Biofilms are the most widespread microbial lifestyle outside microbiology laboratories. As a result, most interactions between bacteria and bacteriophages will likely take place within these complex structured communities. Furthermore, there are multiple examples in which phages affect biofilm development [15]. For instance, prophages in *Shewanella oneidensis* MR-1 enhance matrix accumulation by releasing extracellular DNA (eDNA) [16]. Other temperate phages, however, participate by triggering biofilm dispersal [17, 18] or structural development [19]. There are also some examples involving virulent phages at low concentrations. Although research regarding this phenomenon remains scarce, we do know that its underlying mechanisms are diverse and depend on the specific phage–host pair. Indeed, a study reported that phage predation resulted in enhanced biomass in *Pseudomonas aeruginosa*, *Salmonella enterica*, and *Staphylococcus aureus* [20]. In the first example, this phenotype was due to the selection of strong biofilm-forming mutants, while nonevolutionary mechanisms lay behind the increase observed in the latter two species. Additionally, Tan et al. [21] determined that phage KVP40 promoted cell aggregation in *Vibrio anguillarum* PF430-3, whereas infection of strain BA35 by phage Φ H20 decreased the attached biomass. Previously, we observed that low-level predation by phage phiIPLA-RODI resulted in increased adhered biomass in *S. aureus* IPLA1 due to eDNA accumulation in late stages of biofilm development [22]. Also, cells in the infected biofilms remained susceptible to the phage and displayed major transcriptional changes compared to uninfected biofilms. Indeed, 1063 genes exhibited differential regulation, including 76 genes that suggested an activation of the stringent response. This response is activated by the alarmone (p)ppGpp under different stress conditions, including amino acid starvation, carbon source starvation, depletion of fatty acids, and osmotic stress. The stringent response is known to play a

Table 1 *S. aureus* strains used in this study.

Strain	Description	Reference
IPLA1	Dairy industry surface	[43]
IPLA15	Meat industry surface	[43]
RN450	Derivative of strain NCTC8325	[44]
ISP479r	Derivative of strain NCTC8325	[45]
Newman	Wild type	[46]
<i>rsh_{syn}</i> (Newman-86)	Newman with deletion of nucleotides 942 to 950 of <i>rsh</i> gene	[37]
compl (Newman-86-199)	<i>rsh_{syn}</i> complemented with full-length <i>rsh</i>	[47]

role in different phenotypes such as entry into the stationary phase, biofilm development, virulence, and even antibiotic tolerance [23–26]. Here, we set out to unravel the mechanisms behind the changes in biofilm architecture and transcriptional profile associated to phage pressure.

Materials and methods

Bacterial strains, bacteriophages, and culture conditions

All bacterial strains used are shown in Table 1. *S. aureus* cultures were routinely grown in TSB (Tryptic Soy Broth, Scharlau, Barcelona, Spain) with shaking or on Baird-Parker agar plates (AppliChem, Germany) at 37 °C. Phage phiIPLA-RODI was propagated on *S. aureus* IPLA1 as previously described [27]. Phage titer was determined by using the double-layer technique using *S. aureus* IPLA1 as a host strain [28]. To assess the stability of phiIPLA-RODI particles at different pH values, a phage suspension was diluted in TSB adjusted by adding 0.1 N HCl to a pH of 7, 6, 5, 4.75, or 4.5 at a final titer of 1×10^8 PFU/ml and incubated for 2 h at 37 °C. These phage suspensions were then titrated as indicated above.

Biofilm formation assays

Biofilms were developed in 12-well microtiter plates (Thermo Scientific, NUNC, Madrid, Spain) as previously described [22]. Briefly, cell suspensions containing 10^6 CFU/ml were prepared by diluting overnight cultures in fresh medium. Depending on the experiment, the medium used was TSB (TSB-7), TSB supplemented with 0.25% glucose (TSBG) or TSB adjusted at a pH of 6 (TSB-6). Each well was inoculated with 1 ml from this suspension and 1 ml of fresh medium containing different phage titers. These plates were incubated at 37 °C for 3, 5, 7, 9, or 24 h. Following incubation, the planktonic phase was removed

and serially diluted to determine viable cell counts and free phage titer. Additionally, the pH of the planktonic phase was monitored by using a calibrated pH meter. The adhered phase was also recovered after two washing steps by adding 1 ml of PBS and scraping with a sterile pipette tip. The number of viable cells in the biofilm was then determined by serial dilutions followed by plating. In both phases (planktonic and biofilm), the number of free phages and infectious phage particles stored inside cells (cell-associated phages) was determined as previously described [29]. Briefly, all samples were centrifuged at $10,000 \times g$ for 3 min. To estimate the number of free viral particles, the supernatant was then filtered ($0.45 \mu\text{m}$; VWR, Spain) and titrated as described above. In turn, the pellets were resuspended in $500 \mu\text{l}$ of PBS and cells were lysed by adding $50 \mu\text{l}$ of chloroform in order to release the phage particles. Next, samples were vortexed for 30 s and subsequently centrifuged to remove the cell debris. The supernatant was then filtered and used to estimate the number of cell-associated phages by the double-layer technique.

To estimate the eDNA content of the biofilm matrix, 24-h biofilms were treated with 1 ml of $200 \mu\text{g/ml}$ DNase I in activity buffer (150 mM NaCl and 1 mM CaCl_2) or buffer alone for 1 h at 37°C . After removal of this treatment, the total attached biomass was quantified by crystal violet staining as described previously [30]. Comparison of biomass data between DNase-treated wells and control wells allowed estimation of the biofilm eDNA content. To test the effect of the combination between DNase and phage RODI, 24-h preformed biofilms were treated with 10^9 PFU/well of phiPLA-RODI with or without DNase for 24 h at 37°C . Afterwards, the number of viable cells and phage particles were determined by serial dilution, and total biomass was estimated by crystal violet staining.

Reactivation of the lytic cycle

Phage-infected biofilms were allowed to develop as described above using an initial phage titer of 10 PFU/well (MOI of 10^{-5}). After incubation for 24 h at 37°C , the attached cells were harvested and resuspended in 5 ml of fresh TSBG. This suspension was then incubated without shaking at 37°C and aliquots were taken at 0, 10, 30, and 45 min. The number of free phages and cell-associated phage particles (those found inside unlysed infected cells) was determined as described above.

Monitoring phage propagation under shaking conditions

Overnight cultures of strain IPLA1 were diluted to obtain a suspension containing 1×10^6 CFU/ml in different media, namely TSBG, or TSB-7, and then combined 1:1 with a

phage dilution containing 10 PFU/ml prepared in the same growth media. These samples were subsequently incubated at 37°C under shaking, and samples were taken at 3, 5, 7, and 24 to determine the phage titer and pH as described above.

Phage–host dynamics simulation model

A computational framework in Python 3 was developed to simulate formation of a *S. aureus* biofilm in the well of a 12-well plate under different levels of phage pressure throughout a 24-h period (for further details, please see Supplementary file 1). To do that, the script recalculated every 30 min the environmental pH, as well as the size of three different populations in the biofilm and the planktonic phase: free phage particles, newly infected bacterial cells, and uninfected susceptible cells. Several parameters (bacterial growth rates, phage propagation and pH-stability rates, and rate of pH decrease) were calculated from experimental data. To do that, the number of cells and free phage particles were determined at different time points for samples representing different starting infection levels (starting titers of 0, 1, 10, 100, 1000, and 10,000 corresponding to MOIs of 0 , 10^{-6} , 10^{-5} , 10^{-4} , 10^{-3} , and 10^{-2}). The data obtained in the uninfected samples were used to calculate the growth rate of the bacterial population, as well as the evolution of pH in the growth medium (Supplementary file 1, Figs. A and B). Additionally, phage propagation rates and phage pH-stability rates (the proportion of the phage population that survives at a given pH value) were determined based on the data obtained with an initial MOI of 10^{-5} . Conversely, the probability of infection rates (defined as the number of infected cells per infective viral particle) at different growth stages were estimated computationally in order to maximize the goodness of fit of the model.

Transcriptional analysis

Samples from synchronized infection experiments, those in which most cells are simultaneously undergoing the lytic cycle, were obtained by growing bacterial cultures in TSBG with aeration up to an $\text{OD}_{600} \sim 1.0$ and then infecting them or not with phage phiPLA-RODI (MOI 10). For RNA preparation, 0.5-ml samples were taken at 10 and 20 min postinfection, before the onset of cell lysis. Prior to storage at -80°C , these samples were pelleted at $10,000 \times g$ for 3 min.

To obtain RNA from sessile cells, biofilms were developed for 3, 5, 7, or 24 h without phage (MOI of 0) or by using different initial subinhibitory MOIs (ranging from 10^{-5} to 1000) depending on the strain. After biofilm formation, the first step involved removing the planktonic phase and

washing the attached cells with PBS. Then, cells were scraped from the well in 0.5 ml PBS mixed with 1 ml of RNA protect (Qiagen) and incubated at room temperature for 5 min, subsequently pelleted at $5000 \times g$ for 10 min and further stored at -80°C .

After thawing the samples on ice, RNA purification and quality control were performed according to the protocol described previously [22]. Transcriptional analysis was performed by RT-qPCR as described by Fernández et al. [22]. Three biological replicates, each repeated in duplicate, were analyzed for each condition. Fold changes were calculated according to the Ct method. The reference genes were ribosomal 16S rRNA for strains Newman and its derived *rsh_{syn}* mutant, and *rplD* for all the other strains. Statistical analysis was performed by using a two-tailed Student's *t* test and *p* values < 0.05 were considered significant.

Statistical analysis

Unless otherwise indicated, all experiments were performed with three independent biological replicates, each in duplicate. Data were analyzed with one-way or two-way ANOVA and *p* values < 0.05 were considered significant.

Results and discussion

Propagation of phiIPLA-RODI during *S. aureus* IPLA1 biofilm formation

In previous work, we monitored total attached biomass and the evolution of bacterial cell counts in the planktonic phase and the biofilm of *S. aureus* IPLA1 cultures infected with the strictly lytic phage phiIPLA-RODI at a low MOI (10^{-5}), corresponding to an initial inoculum of 10 PFU/well and 10^6 CFU/well [22]. After 24 h of incubation, biomass in infected wells was significantly higher than in control samples. The number of cells in the biofilm and the planktonic phase were, respectively, $5 \times 10^8 \pm 2.65 \times 10^8$ and $1.00 \times 10^8 \pm 9.17 \times 10^7$ CFU/well, and the total phage titer had increased up to 10^6 PFU/well. Yet, there was no information regarding phage propagation dynamics throughout biofilm development to help understand how it relates to the increase in biomass. Here, we set out to examine phage titer evolution during biofilm formation.

The data obtained in these experiments revealed a gradual increase in the total phage titer in the biofilm from the starting inoculum to $\sim 10^4$, $\sim 10^6$, and $\sim 10^8$ PFU/well at 3, 5, and 7 h of incubation, respectively (Fig. 1a). Afterwards, the phage titer declined drastically, being $\sim 5 \times 10^5$ PFU/ml at the 24-h time point. During most of the development, the

number of free and cell-associated phages was quite similar. However, in 24-h biofilms, most phages were stored inside cells. These assembled phage particles might indicate the presence of infected cells in which the lytic cycle paused just before cell lysis. It is known that phage multiplication comes to a halt when the bacterial population enters stationary phase [31]. These “hibernation mode”, in which the viruses are stored inside the cells at different developmental stages, will last until more nutrients allow the lytic cycle to resume.

Phage propagation in the planktonic phase followed the same trend (Fig. 1a). In this case, the number of free phages and cell-associated phages was similar at 3, 5, and 24 h of development, while free phages represented most of the population at 7 h. The greater abundance of free phages compared to cell-associated phages at 7 h post-infection may indicate that phage propagation is slowing down as the bacterial population approaches stationary phase. It is worth noting that phage propagation was slower in the biofilm than in the planktonic phase, which is in good agreement with the idea that structured environments delay phage propagation [8]. Additionally, it appears that the biofilm has a protective effect from phage decay, as most particles were “hidden” inside sessile cells at 24 h of development. One possible explanation for this would be that the latency period of phiIPLA-RODI is longer in the biofilm than in the planktonic phase. Nonetheless, this hypothesis would have to be experimentally confirmed in a subsequent study. Overall, these results show that, after successful propagation during biofilm development, there is a substantial loss of active phage particles between 7 and 24 h of incubation.

Phage inactivation is likely due to acidification of the extracellular milieu by bacterial metabolism end products

After observing the existence of phage inactivation during biofilm formation, we sought to determine the mechanism behind this phenomenon. One possible explanation for the decrease in free phages might be that phage DNA entered the cytoplasm of infected cells, thereby decreasing the number of infective particles in the culture, but could not proceed with the lytic cycle due to bacterial growth arrest or an adverse metabolic state. To test this hypothesis, we followed the release of phage particles (due to completion of the lytic cycle) upon resuspension of mature biofilm cells in fresh medium. The number of free phages and preformed virions stored inside cells was estimated at different time points throughout 45 min of incubation, which is approximately the duration of the phiIPLA-RODI lytic cycle [23]. At the beginning of the experiment, the number of free phages was $2.18 \times 10^4 \pm 1.24 \times 10^4$ PFU/well, while the

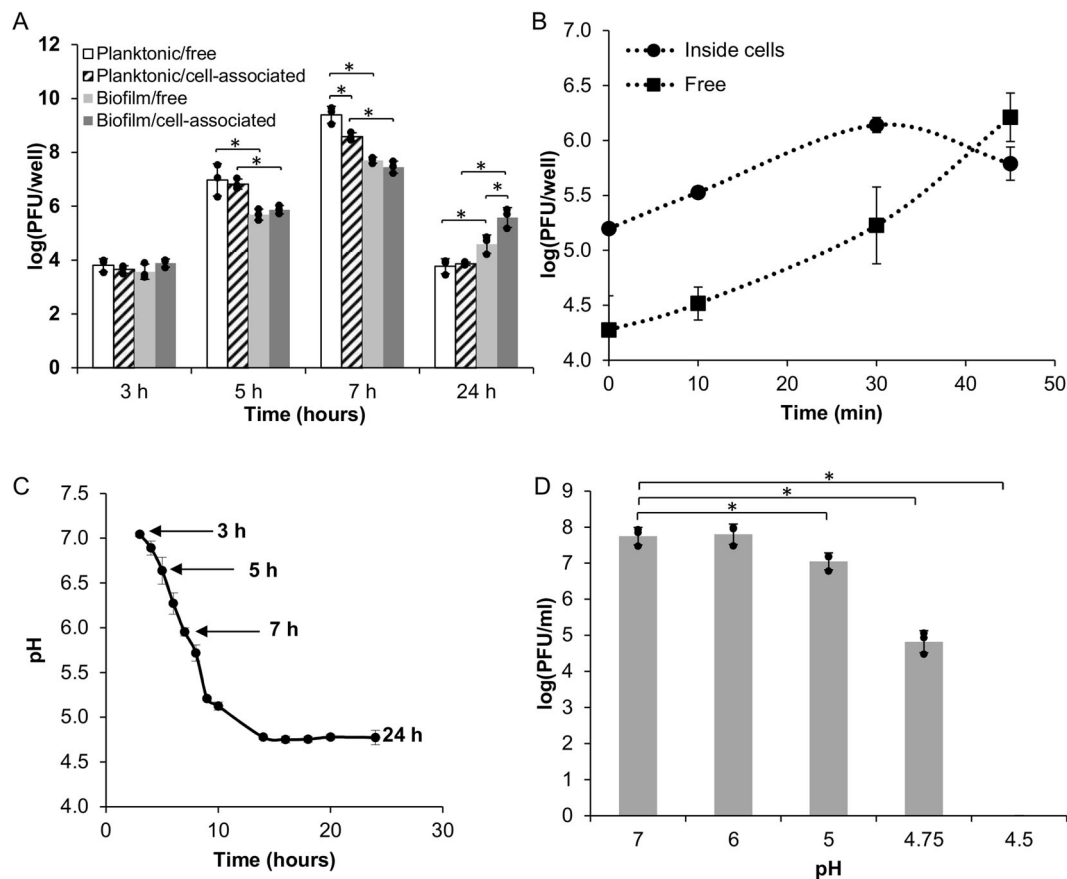


Fig. 1 Analysis of the propagation and inactivation of bacteriophage phiIPLA-RODI during biofilm development of *S. aureus* IPLA1 and the potential role of pH in phage inactivation. **a** Number of free (white and light gray) and cell-associated (striped and dark gray columns) phage particles in the biofilm (light gray and dark gray columns) and the planktonic phase (white and striped columns) at different time points during biofilm development in the presence of an initial inoculum of 10^6 PFU/well and 10^6 CFU/well. **b** Reactivation of the lytic cycle in mature biofilm cells infected with phiIPLA-RODI resuspended in fresh medium and incubated at 37°C for 45 min. The

number of preformed virions inside cells was $1.19 \times 10^5 \pm 8.00 \times 10^4$ PFU/well (Fig. 1b). However, after 45 min, the number of free and cell-associated phage particles increased up to $1.77 \times 10^6 \pm 8.69 \times 10^5$ and $4.81 \times 10^5 \pm 3.72 \times 10^5$ PFU/well, respectively. At this time point, any previously infected cell should have completed the lytic cycle and released the viral progeny. However, the number of phage particles is still much lower than 1×10^8 PFU/well, the phage titer present in the 7-h biofilms, that is, before the start of phage decay. Therefore, it does not appear likely that halted lytic cycles are the only explanation for the sharp reduction in viral particles.

An alternative explanation for the decrease in phage titer might be the selection of resistant mutants that can no longer support phage propagation. However, previous data indicated that cells in the phage-infected biofilms remained susceptible to phiIPLA-RODI [22].

number of free (squares) and cell-associated (circles) phage particles was estimated at different time points throughout incubation. The dotted line has been added only as a guide and does not represent true data points. **c** pH evolution in the growth medium during development of *S. aureus* IPLA1 biofilms in TSBG. **d** Phage titer after incubation of phiIPLA-RODI in TSB medium at different pH values for 2 h at 37°C . The graphs represent the means and standard deviation of three independent biological replicates (averaged from two technical duplicates). Statistical analysis was performed with a one-way ANOVA with post-hoc Tukey's multiple comparison. * p value < 0.05 .

Next, we explored the potential inactivation of phage particles by pH. González-Menéndez et al. [32] had already shown that phiIPLA-RODI stability was lost after 1 h at a pH of 4.5. In *S. aureus*, glucose catabolism produces acetate, which gradually lowers the pH. During biofilm formation in TSBG, the pH dropped from 7 to ~4.75 (Fig. 1c). A 2-h incubation of phage phiIPLA-RODI in TSB at different pH values (7, 6, 5, 4.75, and 4.5) demonstrated phage inactivation at $\text{pH} \leq 5$ (Fig. 1d). Thus, the number of active phage particles after incubation at pH values of 5 and 4.75 had decreased by 0.70 and 2.93 log units, respectively (Fig. 1d). As expected, a pH of 4.5 inactivated the phage below the detection level of 100 PFU/ml (Fig. 1d). Perhaps, instability of the phage particle is related to the fact that the major capsid protein has an isoelectric point of 5.24 according to the program Protein Calculator v3.4 (<http://protecalc.sourceforge.net/>). Thus, when pH decreases below

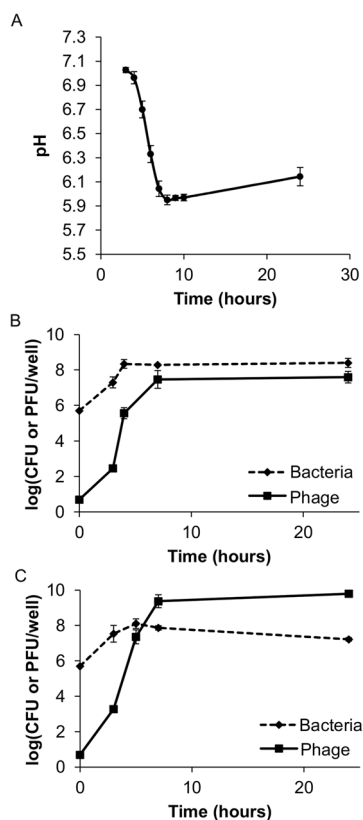


Fig. 2 Biofilm development under predation with an initial MOI of 10^{-5} of phage ϕ IPLA-RODI (10 PFU/well) in TSB-7 for 24 h at 37 °C. **a** The pH of the planktonic phase was monitored throughout the incubation period. Number of viable cells (◆) and phage titer (■) in the biofilm (**b**) or the planktonic phase (**c**) during development. The results represent the average and standard deviation of three independent repeats.

this point, this protein would go from having a negative charge to having a net positive charge. An acidic pH may also lead to phage inactivation by promoting precipitation or aggregation of the viral particles, as has been observed in other phages [33, 34]. Interestingly, Langlet et al. [34] observed aggregation of phage MS2 when the pH was less than or equal to its isoelectric point.

To further confirm the impact of pH on the final phage titer during biofilm development, biofilms infected with ϕ IPLA-RODI (starting MOI = 10^{-5}) were also grown in TSB-7 (TSB with a pH of ~7). In this medium, pH never went below 5.9 and, after reaching that value, it started increasing up to ~6.2 (Fig. 2a). This was likely due to glucose exhaustion and subsequent use of acetate as an energy source. Under these conditions, there was no net decrease in the number of free phage particles between 7 and 24 h of incubation neither in the biofilm (Fig. 2b), nor in the planktonic phase (Fig. 2c). The effect of phage infection in TSB-7 on the bacterial population was also examined. The average number of viable cells in the mature 24-h biofilm was $2.77 \times 10^8 \pm 1.37 \times 10^8$, which is significantly

lower than $7.28 \times 10^8 \pm 1.30 \times 10^8$, the cell counts determined in infected biofilms grown in parallel in TSBG (two-tailed *t*-test, *p* value = 0.014). The difference was also significant in the planktonic phase, where the respective cell counts in TSBG and TSB-7 were $1.13 \times 10^8 \pm 3.29 \times 10^7$ and $1.67 \times 10^7 \pm 3.51 \times 10^6$, respectively (two-tailed *t*-test, *p* value = 0.036). All these findings seem to indicate that acidification of the extracellular environment by accumulation of bacteria-produced acetate is probably the factor behind phage decay. In turn, phage inactivation appears to have a positive impact on the survival of the host population.

In order to establish whether phage decay due to pH was specific to biofilms, phage propagation and decay was monitored in a well-mixed environment in two different media: TSBG and TSB-7. In TSBG, we observed a gradual increase in the number of free phages up to the 7 h time point (Fig. S1). Then, similarly to the results obtained in the biofilm experiments, there was a significant decrease in the phage titer (0.51 ± 0.11 logarithmic units) (Fig. S1). In parallel to this reduction, the pH of the medium declined from 5.93 ± 0.02 to 5.22 ± 0.16 . Under these conditions, phage decay was clearly not as dramatic as during biofilm development. This can be explained by the lesser acidification of the growth medium under constant shaking compared to static incubation. In contrast to these results, there was no significant phage inactivation between 7 and 24 h when cultures were grown in TSB-7, in which pH only decreased from 6.39 ± 0.08 to 6.21 ± 0.05 (Fig. S1). This is in good agreement with the data obtained in the phage inactivation assays, in which no decay was observed when $\text{pH} \geq 6$. Therefore, it does appear that the correlation between environmental pH and phage decay also applies in well-mixed populations, although the greater acidification displayed during biofilm development seems to enhance this effect.

The evolution of pH during biofilm development affects the outcome of ϕ IPLA-RODI predation

Once established that pH was likely responsible for phage inactivation, we tried to better understand how changes in this parameter affect the interplay between ϕ IPLA-RODI and *S. aureus* cells during biofilm development. With this in mind, a numerical simulation model was built to mimic the development of the phage and bacterial populations depending on the environmental pH (Supplementary file 1). Importantly, phage inactivation was modeled as a function of pH (Supplementary file 1). Once established all the data-derived parameters, the model was optimized for the best probability of infection values at different time points for the biofilm and the planktonic phase. When using the optimal probability of infection

values, the goodness of fit for all conditions tested was >0.75 (Fig. S2).

In the simulation, the starting and final pH values were set at 7.0 and 4.75, respectively. Throughout the different steps of the model, pH decreases gradually with bacterial growth. However, due to the deleterious effect of phage predation on bacterial growth, the minimum pH of 4.75 was only observed in the uninfected control, closely followed by 4.95, the final pH achieved with 1 or 10 PFU/well. In turn, infection with 100, 1000, or 10000 PFU/well resulted in final pH values of 5.54, 5.82, and 6.45, respectively. As phage inactivation was set to start at values below 5.55, pH-mediated inactivation of phiIPLA-RODI would only be a factor at the lowest starting phage concentrations (1, 10, and 100 PFU/well). In order to determine how much the final pH would affect infection dynamics, the model was run setting the lowest pH value at 5.9, 5.5, 5.0, and 4.75 with starting titers of 10 and 100 PFU/well (MOIs: 10^{-5} and 10^{-4}). These conditions would mimic, for example, small differences in the availability of glucose in the growth medium. As can be seen in Fig. 3, the most obvious change in both the biofilm and the planktonic phase at both starting MOIs is the increase in the final phage titer with higher pH values due to a lesser phage inactivation (Fig. 3). Indeed, the total phage titer (planktonic and biofilm) with an initial inoculum of 10 PFU/well was 1.15×10^6 , 1.26×10^7 , 7.90×10^8 , and 7.32×10^9 for final pH values of 4.75, 5.0, 5.5, and 5.9, respectively. In turn, the total phage for a starting inoculum of 100 PFU/well was 8.36×10^9 and 7.32×10^{10} for pH values ≤ 5.5 and 5.9, respectively. Looking more closely at the graphs, it is also apparent that pH affects bacterial population survival. For instance, when the starting phage titer was 10, no decrease in the biofilm cell population was observed at final pH values of 4.75, 5.0, and 5.5, but a slight decrease in the number of viable uninfected cells was predicted if the pH remained over 5.9. At the same starting titer, phage predation marginally reduced the number of cells in the planktonic phase at all pH values, although an even greater impact was observed in the absence of phage inactivation at a pH of 5.9. When the model was run with a starting phage titer of 100 PFU/well, the most notable changes were observed for the biofilm population. In turn, the outcome in the planktonic phase was independent of the final pH due to the elimination of susceptible uninfected cells prior to the outset of phage inactivation. Surface-attached susceptible cells, however, were only eradicated when the final pH was set at 5.9.

Besides the final pH value, another factor that would have an impact on phage infection outcome would be the timing of phage inactivation start in relation to biofilm development dynamics. To examine this possibility, the

model was run with a starting pH of 6 and a final pH of 5 without changing any other parameters. With a lower initial pH, it would be expected to reach values that lead to phage inactivation at an earlier time point. The results obtained under these conditions showed that, for a starting titer of 10 PFU/well, phage inactivation started ~ 360 min after inoculation (Fig. 4). In contrast, phage inactivation did not begin until ~ 480 min of incubation when the initial pH was 7 (Fig. 3). As a result of this difference, with a lower initial pH, the starting phage titer necessary to eliminate the susceptible bacterial population in both phases (biofilm and planktonic phase) was 10^5 PFU/well (Fig. 4) instead of 1000 PFU/well, as was predicted for an initial pH of 7 (Fig. S2). That said, the model predicted that bacteria in the planktonic phase could be killed with a lower titer (1000 PFU/well) even when the starting pH was 6 (Fig. 4), suggesting that cells in the biofilm might, to some extent, be protected from viral attack. Next, we examined experimentally whether biofilm development in TSB medium adjusted at a pH of 6 (TSB-6) had an impact in bacterial survival to a viral challenge. The results of these assays showed that inhibition of visible bacterial growth in TSB-6 required an initial phage titer of 10^6 PFU/well, thereby reflecting the trend predicted by the model (data not shown). Nonetheless, it must be taken into account that this prediction did not consider that a more acidic pH during early growth stages might affect the bacterial growth rate or the probability of infection (for instance, by altering the number of phage receptors on the cell surface). These additional factors may, at least to some extent, explain the difference between the model and the experimental data, and deserve to be explored in a subsequent study. Overall, all these results indicate that both the timing and the degree of phage inactivation by pH might have an impact on bacterial population survival.

A mildly acidic pH is required for the development of phage-promoted eDNA-enriched biofilms

Our subsequent objective was to determine whether pH also had an effect on the development of the DNA-rich phenotype displayed upon low-level phage infection. As is mentioned above, infection with a starting phage number of 10 PFU/well led to greater killing in TSB-7 than in TSBG. Additionally, upon infection by phiIPLA-RODI, the total biofilm biomass decreased in TSB-7 while it increased in TSBG (Fig. 5a). In contrast, when biofilms were formed in TSB-6 certain concentrations of phage did lead to a biofilm increase (Fig. 5a). Nonetheless, an inoculum of 10^4 PFU/well was necessary to observe this phenotype, as opposed to the 10 PFU/well that promoted biofilm accumulation in TSBG. This correlates with the

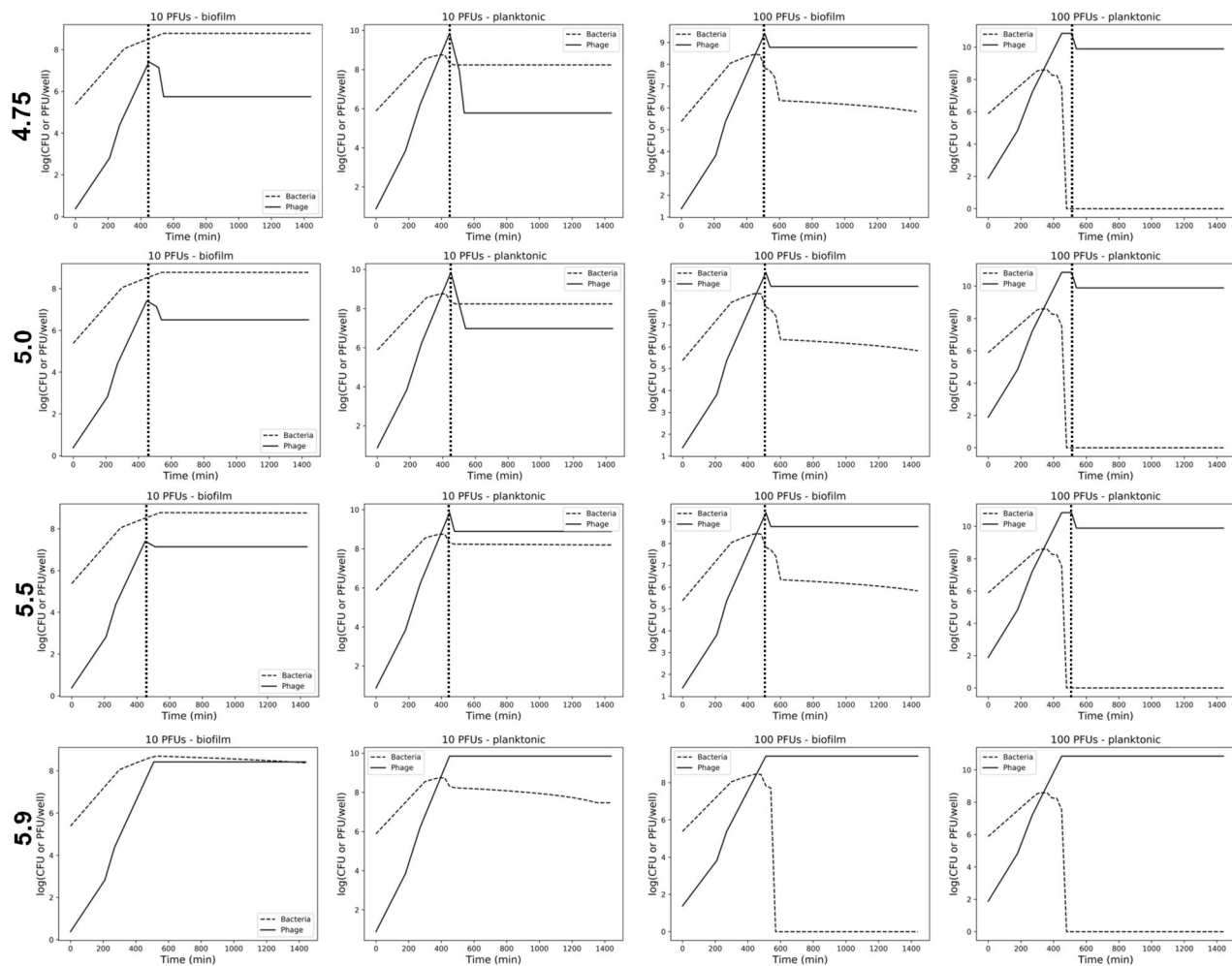


Fig. 3 Output of the optimized phiIPLA-RODI infection model for different starting phage concentrations (10 and 100 PFU/well) in the biofilm and the planktonic phase when the lowest possible pH value was set at 4.75, 5.0, 5.5, or 5.9. The starting number of cells was always set at 10^6 CFU/well, and the initial pH was set at 7. The

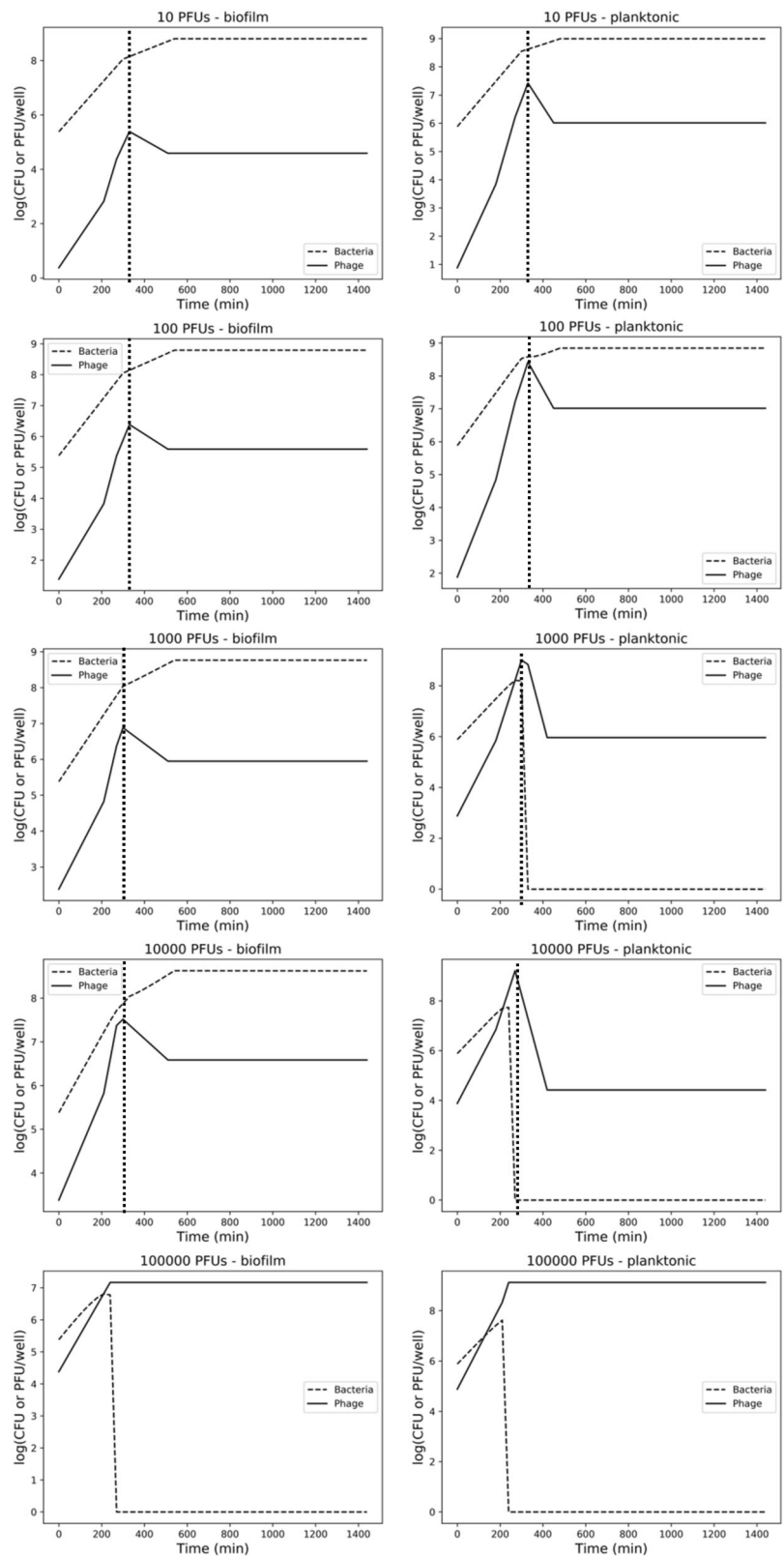
bacterial and phage populations are represented by a discontinuous line and a continuous line, respectively. The vertical dotted lines indicate the point right before the start of phage inactivation, that is, before the pH goes below 5.55.

fact that a higher initial MOI is required to achieve growth inhibition in this medium, as is mentioned above. Indeed, Fernández et al. [22] had already observed that a higher initial phage titer was necessary to promote biofilm development in strain IPLA15, which was less susceptible to phiIPLA-RODI than IPLA1. Altogether, these results suggest that two key conditions are required for the formation of eDNA-rich biofilms in these two strains, namely a mildly acidic environment and phage infection of a fraction of the bacterial population. It has been well established that biofilm formation in *S. aureus* is favored at pH values around 5, as mildly acidic conditions favor electrostatic interactions between the negatively charged cell surface, positively charged moonlighting cytoplasmic proteins and the negatively charged eDNA [35, 36]. It is possible that some strains do not release sufficient cytoplasmic proteins and/or DNA to form the extracellular

matrix, and may benefit when these molecules are released through partial cell lysis of the population by phage predation. Considering the data described above, it becomes apparent the importance of ensuring that pH does not go below 5 when using phage phiIPLA-RODI, and potentially other pH-sensitive phages, to treat *S. aureus* biofilms. However, if it is necessary to use this phage in acidic environments, the phage preparation could be supplemented with DNase. Indeed, treatment of preformed biofilms with 10^9 PFU/well of phiIPLA/RODI supplemented with DNase I prevented the increase in biomass observed during treatment with the phage alone (Fig. 5b). Furthermore, there was a reduction in viable cell counts in the attached phase compared to an untreated sample despite the existence of phage inactivation (Fig. S3). This phenomenon is probably linked to increased biofilm dispersion through degradation of the matrix by the enzyme.

Fig. 4 Output of the optimized phiPLA-RODI infection model for different starting phage concentrations (10, 100, 1000, 10^4 , and 10^5 PFU/well) in the biofilm and the planktonic phase when the starting pH value was set at 6 and the lowest pH value reached during growth was set at 5.

The starting number of cells was always set at 10^6 CFU/well. The bacterial and phage populations are represented by a discontinuous line and a continuous line, respectively. The vertical dotted lines indicate the point right before the start of phage inactivation, that is, before the pH goes below 5.55.



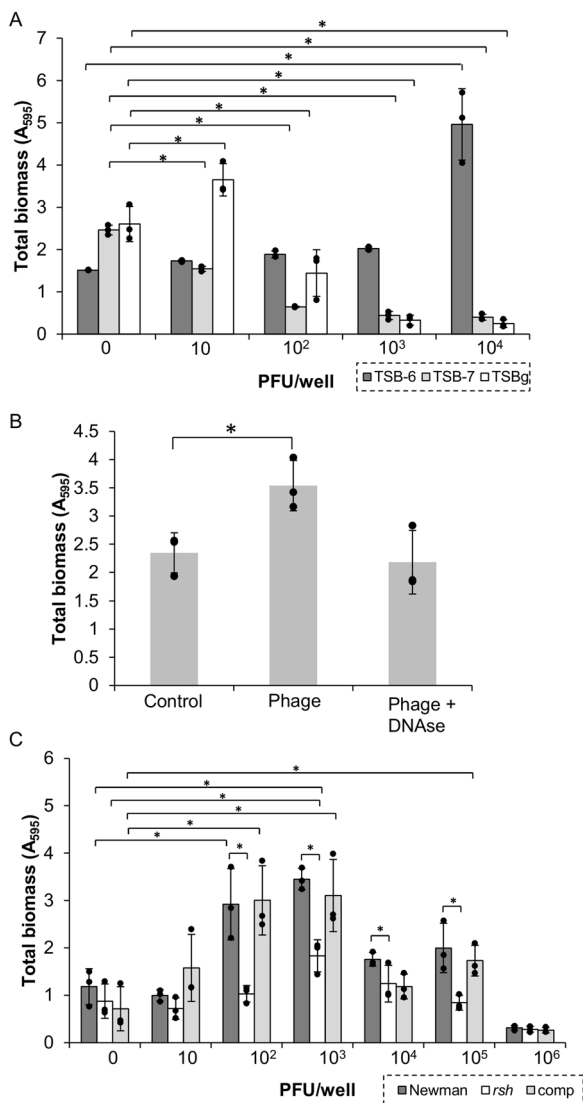


Fig. 5 Impact of phage predation on biofilm formation and elimination of *S. aureus*. Total biomass was determined by crystal violet staining by reading absorbance at 595 nm. **a** Biofilm formation of *S. aureus* IPLA1 in different media (TSBG, TSB-7, and TSB-6, respectively represented by white, light gray and dark gray bars) and infected with different starting concentrations of phage phiIPLA-RODI. Biofilms were allowed to develop for 24 h and then were stained with crystal violet. For each medium, biomass of the treated samples was compared to that of the control. **b** IPLA1 biofilms were formed in TSBG for 24 h at 37 °C and then treated for another 24 h with 10⁹ PFU/well of phage phiIPLA-RODI with or without 100 µg/ml DNase I. Biomass of the treated samples was then compared to that of the control. **c** Effect of *rsh* mutation on biofilm formation for 24 h at 37 °C of *S. aureus* Newman in the presence of increasing initial titers of bacteriophage phiIPLA-RODI. Dark gray and white bars represent the wild-type Newman strain and the *rsh_{syn}* mutant strain, respectively. Light gray bars correspond to the complemented *rsh* strain. For each strain, biomass of the treated samples was compared to that of the control. Also, for each phage concentration, biomass of the wild type was compared to that of the other two strains. All graphs represent the means and standard deviation of three independent biological replicates (averaged from two technical duplicates). Statistical analysis was performed with a one-way (a, b) or two-way (c) ANOVA with post-hoc Tukey's multiple comparison. **p* < 0.05.

These results are relevant in the context of phage therapeutic applications. Indeed, it seems to be important to establish whether the pH in a given environment is mildly acidic prior to phage administration and, if that is the case, DNases could be used in combination with the phage to prevent increased biofilm formation.

The transcriptome of infected biofilms varies depending on the pH

Besides altering biofilm composition, development under low phage predation in TSBG also led to changes in the transcriptome [22]. Here, we sought to study the underlying causes of this phenomenon. In order to do that, we selected five genes that exhibited phage-related dysregulation in 24-h IPLA1 biofilms, and analyzed their expression under different conditions involving phage infection (Table 2). These genes were interesting for different reasons. For example, *rsh*, encoding a bifunctional (p)ppGpp synthase and hydrolase, was chosen as an indicator of activation of the stringent response, which has been known to participate in biofilm formation. In turn, *clpC*, an ATP-binding subunit of the ATP-dependent Clp protease, was selected because we observed downregulation of multiple *clp* protease genes, which are known to exert regulatory roles in diverse cellular processes. The major autolysin-encoding gene, *atlA*, and *icaA*, which participates in the synthesis of extracellular polysaccharide, were analyzed because of their participation in biofilm formation. Indeed, eDNA release due to activity of AtIA is very important, at least in early biofilm stages. Finally, *crtP*, one of the genes involved in the production of the carotenoid pigment staphyloxanthin, indicates activation of the sigma B regulon, which plays a role under different stress conditions, including biofilm formation. In 24-h biofilms formed in TSBG, four of these genes (*rsh*, *atl*, *crtP*, and *icaA*) were upregulated during infection with phage phiIPLA-RODI, whereas *clpC* was downregulated (Table 2).

First, we analyzed whether the expression of these genes changes as a result of phage replication inside the host cells. To do that, it is important to synchronize the lytic cycle in practically all the cells in the population by using an MOI that leads to complete lysis of the culture within one lytic cycle, which is more easily achieved by infecting a liquid culture rather than a biofilm. In the case of phiIPLA-RODI, this process has been estimated to take ~50 min [15], and was attained by infecting the bacterial culture with an MOI of 10 (Fig. S4). Under these experimental conditions lysis started after 20 min of incubation. Therefore, samples for transcriptional analysis were taken at 10 min (time point 1) and 20 min (time point 2) after infection start and compared to a noninfected control. The results obtained in this experiment indicated that expression of all the analyzed

Table 2 Gene expression changes associated to phage infection of *S. aureus* cultures under different conditions.

Conditions	Genes*				
	<i>rsh</i>	<i>clpC</i>	<i>atl</i>	<i>crtP</i>	<i>icaA</i>
IPLA1-Biofilm TSBG 24 h (MOI: 10 ⁻⁵ vs MOI: 0)	33.9 ± 17.2	-5.0 ± 1.0	31.9 ± 18.8	25.6 ± 14.8	4.1 ± 0.7
IPLA1-Sync. inf. TSB-7 10 min (MOI: 10 vs MOI: 0)	-16.8 ± 8.1#	-10.7 ± 7.1#	-6.4 ± 2.1#	-3.9 ± 1.6#	-3.5 ± 2.3
IPLA1-Sync. inf. TSB-7 20 min (MOI: 10 vs MOI: 0)	-54.3 ± 40.5#	-18.0 ± 12.2#	-12.4 ± 1.6#	-43.6 ± 2.1#	-4.3 ± 2.3
IPLA1-Biofilm TSB-7 (MOI: 10 ⁻⁵ vs MOI: 0)	-1.7 ± 0.2#	-4.2 ± 1.0#	-7.1 ± 0.9#	-1.7 ± 0.3#	1.1 ± 0.5
IPLA1-Biofilm TSBG 3 h (MOI:10 ⁻⁵ vs MOI: 0)	-1.9 ± 1.3	1.1 ± 1.2	-2.6 ± 1.5	-1.7 ± 0.9	1.6 ± 1.0
IPLA1-Biofilm TSBG 5 h (MOI:10 ⁻⁵ vs MOI: 0)	-1.5 ± 0.5	-1.8 ± 0.4	1.0 ± 0.1	-1.7 ± 0.5	1.0 ± 0.4
IPLA1-Biofilm TSBG 7 h (MOI:10 ⁻⁵ vs MOI: 0)	-1.3 ± 0.2	-2.0 ± 0.3	1.1 ± 0.3	-2.4 ± 1.9	-2.1 ± 0.5
IPLA15-Biofilm TSBG 24 h (MOI:0.01 vs MOI: 0)	2.9 ± 0.9#	0.9 ± 0.3	1.1 ± 0.4	1.1 ± 0.1	1.2 ± 0.2
RN450-Biofilm TSBG 24 h (MOI:1000 vs MOI: 0)	-1.2 ± 0.1	-1.2 ± 0.3	-1.6 ± 0.4	1.6 ± 0.4	1.2 ± 0.1
ISP479r-Biofilm TSBG 24 h (MOI:0.001 vs MOI: 0)	-1.8 ± 0.7	-2.3 ± 0.5#	1.1 ± 0.2	-2.9 ± 0.6#	-2.3 ± 0.4#
Newman-Biofilm TSBG 24 h (MOI:0.01 vs MOI: 0)	31.4 ± 0.94.1#	1.0 ± 0.1	26.8 ± 4.1#	10.4 ± 7.1#	1.6 ± 0.7
<i>rsh_{syn}</i> -Biofilm TSBG24h (MOI:0.01 vs MOI: 0)	2.4 ± 2.4	-1.7 ± 1.0	2.9 ± 2.7	2.4 ± 1.9	-9.1 ± 7.8

**atl* (bifunctional autolysin AtlA), *rsh* (bifunctional (p)ppGpp synthase and hydrolase), *clpC* (ATP-binding subunit of ATP-dependent Clp protease), *crtP* (diapolycopene oxygenase involved in staphyloxanthin synthesis), and *icaA* (poly-β-1,6-N-acetyl-D-glucosamine synthase/exopolysaccharide synthesis).

#*p* value < 0.05; cells in gray correspond to overlaps with the dysregulation observed in infected 24-h biofilms grown in TSBG; Sync. inf. stands for synchronized infection.

genes, except *icaA*, was significantly lower in phage-infected samples at both time points (Table 2). Therefore, it is clear that the host genes do exhibit changes in the transcriptome during infection by phiIPLA-RODI, although they do not resemble those previously observed in infected biofilms.

Next, we examined gene expression trends in 24-h phage-infected biofilms grown in TSB-7 instead of TSBG to assess the influence of pH on the transcriptional pattern of infected biofilms. We found that infected biofilm cells grown in TSB-7 displayed a lower expression of *rsh*, *clpC*, *atl*, and *crtP*, but not *icaA*, compared to the uninfected samples (Table 2). These results are very similar to the ones observed during synchronized infection (Table 2). Therefore, it is plausible that they reflect the predominance of infected cells in the biofilm. Indeed, the data presented above suggest that the biofilms formed in TSB-7 contain a higher number of phage-infected cells than those developed in TSBG, which actually seems likely given the viable cell count data presented above (Fig. 2). Nonetheless, we cannot discard the possibility that the transcriptome of phage-infected cells varies depending on environmental pH. However, carrying out a synchronized infection experiment at a low pH is challenging due to phage inactivation under these conditions, which would make it necessary to use a very high MOI. Overall, with the available information, it seems that the transcriptional pattern displayed by phage-infected biofilms does not appear to be associated to the development of the lytic cycle in infected cells, and vary depending on the final pH of the growth medium.

The transcriptional pattern of phage-infected biofilms is linked to the changes in structure and composition

The data presented above suggest that the transcriptional differences observed in TSBG-grown phage-infected mature biofilms may not be a direct result of the development of the lytic cycle inside the infected cells, although this remains to be demonstrated. With these results in mind, the next step was to determine if these changes had already started at an earlier time point during biofilm formation. To do that, gene expression of samples from biofilms infected with phiIPLA-RODI at an MOI of 10⁻⁵ were taken at different time points (3, 5, and 7 h) and compared to those developed without phage pressure. We observed that there were no significant differences between infected and non-infected biofilms at 3, 5, and 7 h of development (Table 2). Data obtained in a previous study had already shown that there were no significant differences regarding the amount of attached biomass between infected and uninfected samples at these three time points [22]. Notably, the pH at these time points remained greater than or equal to 5.9, suggesting again the need for a lower pH to observe the phenotypic and transcriptional changes associated to phage infection of *S. aureus* IPLA1.

Subsequently, we aimed to establish whether the gene expression trends of infected biofilms were linked to the increased biofilm phenotype. Previous work had shown that low-level infection of strains IPLA1 and IPLA15 led to a greater amount of attached biomass, which in IPLA1 was

shown to be due to a greater eDNA content [22]. Here, we assessed whether this was also the case for other three *S. aureus* strains: Newman, RN450 and ISP479r. Biofilms of these strains were formed without phage pressure or infected with a starting subinhibitory phage titer for transcriptional analysis (100 times below the lowest titer inhibiting bacterial growth). These titers were 10^3 PFU/well (MOI = 10^{-3}), 10^4 PFU/well (MOI = 10^{-2}), 10^4 PFU/well (MOI = 10^{-2}), and 10^9 PFU/well (MOI = 1000) for strains ISP479r, Newman, IPLA15 and RN450, respectively. The results obtained indicated that there was no significant increase in biofilm formation for strains RN450 or ISP479r at subinhibitory phage concentrations (Fig. S5). Additionally, in these two strains there was a significant eDNA content in the matrix of both infected and noninfected biofilms, as they were all sensitive to DNase treatment. In contrast, the phenotype of biofilms formed by strain Newman was more similar to those of IPLA1 and IPLA15 (Fig. S5). Infected biofilms exhibited a greater amount of total biomass than their phage-free counterparts. Moreover, while the control biofilms were not affected by DNase treatment, biofilms grown in the presence of phiIPLA-RODI were DNase-sensitive, indicating that they had a significant eDNA content. Next, transcriptional analysis of these biofilms was performed by RT-qPCR. The results of these tests showed that, like IPLA1 (Table 2), both IPLA15 and Newman exhibited an upregulation of gene *rsh* in infected biofilms, and the latter also had a higher expression of the autolysin-encoding gene *atl* and staphyloxanthin biosynthesis gene *crtP* (Table 2). However, neither strain displayed a dysregulation of genes *clpC* or *icaA*. By contrast, strain RN450 did not show any overlaps with the transcriptional trends observed in IPLA1 mature biofilms upon phage infection (Table 2). In strain ISP479, the only overlap was downregulation of *clpC*, but there was no significant change in the expression of *rsh* or *atl*, and genes *crtP* and *icaA* displayed the opposite trend to that observed in IPLA1 (Table 2). Overall, these findings show that a higher expression of *rsh* is linked to the display of a biofilm-architectural change involving an increase in DNA content as a result of phage infection under acidic conditions. In *S. aureus*, the product of *rsh* consists of two domains respectively involved in the synthesis and hydrolysis of the alarmone (p)ppGpp, which controls the stringent response [37]. This result is interesting considering that a significant fraction of the genes dysregulated in phage-infected biofilms of strain IPLA1 were part of the stringent response [22]. The regulatory cascade activated by (p)ppGpp is known to participate in biofilm development in different microorganisms. For example, *Vibrio cholerae* stringent response mutants exhibited a lesser ability to form biofilms than the wild-type strain [26]. The stringent response regulator DksA played a major role in biofilm formation of

Salmonella Typhimurium [38], whereas accumulation of inorganic polyphosphate inhibited biofilm formation in *Mycobacterium tuberculosis* [39]. In *Pseudomonas putida*, the stringent response leads to biofilm dispersal [40]. Therefore, it is possible that this response also contributes to biofilm regulation in *S. aureus*, although its precise role is yet to be defined. Altogether, it seems that the distinct transcriptome of phage-infected biofilms of some *S. aureus* strains, in particular the activation of the stringent response, go together with the development of enhanced DNA-enriched biofilms.

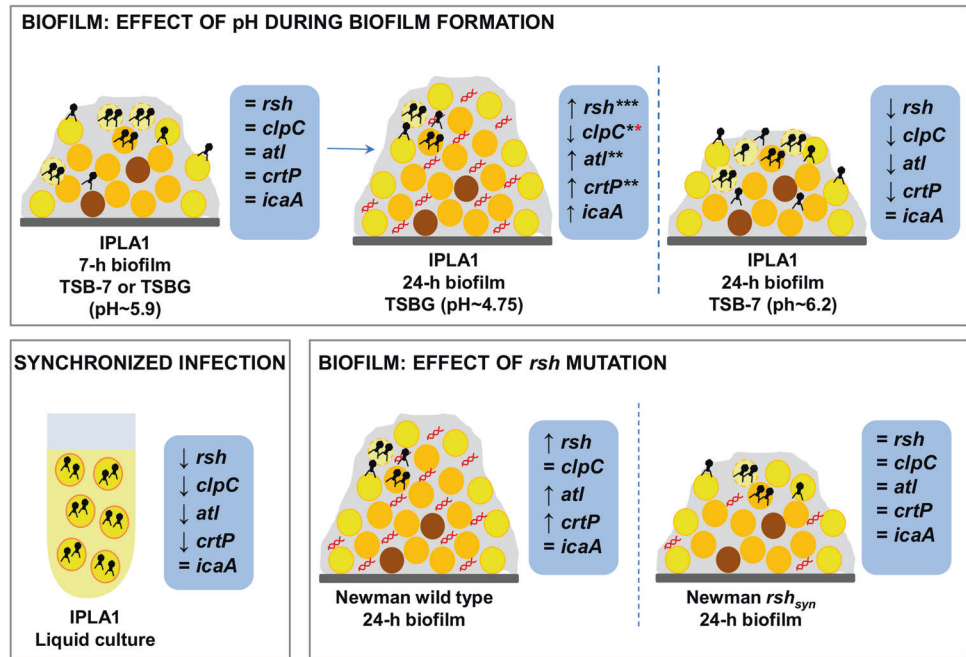
Mutation of *rsh* partially impairs phage-promoted increase in biofilm formation

Taking into account the data presented above, we sought to determine whether (p)ppGpp synthesis mediated by the RSH protein participated in the observed biofilm phenotype. To do that, we used a mutant derived from strain Newman, previously obtained by Geiger et al. [39], carrying a deletion in the synthase domain, while retaining the essential hydrolase activity. First, we compared phage susceptibility of the mutant strain with that of the wild type. Our results showed that visible growth inhibition was achieved with the same phage titer for both strains, that is, 10^7 PFU/ml. However, low-level predation by phage phiIPLA-RODI did not lead to as much biomass induction as in the wild type with some of the concentrations tested (Fig. 5c). Moreover, enhancement of biofilm formation by the phage in a complemented strain was similar to that observed in the wild type, as no significant difference in total biomass was observed between these two strains at any phage concentration (Fig. 5c). Next, RT-qPCR analysis showed that the *rsh_{syn}* mutant did not display a significant upregulation of genes *rsh*, *atl*, and *crtP* observed in the Newman wild type (Table 2, Fig. 6). Therefore, it is possible that activation of the stringent response is involved in upregulation of these genes. Altogether, these results suggest that the increased DNA content in the wild type may not be due exclusively to cell debris released by phage lysis, but also to partial lysis of the population through other mechanisms like autolysis. Previous studies had shown that different staphylococcal proteins with autolytic activity, AtlA and Sle1, participate in biofilm formation by contributing to the accumulation of eDNA in the extracellular matrix [41, 42].

Concluding remarks

Some of the preferred niches of *S. aureus*, including human skin, have a mildly acidic pH, which favors biofilm formation in this opportunistic pathogen. However, a low pH is not enough for many strains, which seem to be poor

Fig. 6 Schematic summary of the effect of phiIPLA-RODI infection on *S. aureus* gene expression under different conditions. **a** Biofilms formed by strain IPLA1 in TSB-7 or TSBG at different time points. Asterisks represent the number of *S. aureus* strains that exhibited the same transcriptional trends as strain IPLA1 (black: strain showing biomass increase under phage predation; red: strain not showing biofilm increase under phage predation). **b** Synchronized phage infection in a liquid culture. **c** 24-h biofilms formed by strain Newman and its derived *rsh* mutant in TSBG.



biofilm formers under in vitro conditions. Yet, our results suggest that this may not necessarily be the case in their natural environment. Indeed, partial lysis of the population due to phage infection seems to allow the survivors to form stable and strong DNA-rich biofilms by providing additional extracellular material. Moreover, these changes in biofilm structure and composition alter the population transcriptional profile. This population reprogramming also appears to contribute to biomass accumulation, presumably through a mechanism that relies on activation of the stringent response. Nonetheless, further work should confirm this link and unearth the specific mechanisms involved. At the same time, development in a mildly acidic environment contributes to phage–host coexistence through partial inactivation of the phage population. This would, in turn, keep bacterial killing under control and prevent extinction of the host population. It must be noted, however, that this phenomenon is not desirable in the context of phage therapy. Indeed, it seems that use of phiIPLA-RODI, and perhaps other staphylococcal phages, in mildly acidic environments like the human skin would require adding a pH-raising agent or DNase to prevent increased biofilm development. Overall, environmental pH can modulate the ability of a bacterial population to thrive by fine tuning the effects of phage attack in a way that ultimately benefits both the phage and the host, and by contributing to enhanced biofilm formation.

Acknowledgements We would like to thank Dr. J.R. Penadés and Dr. N. Quiles-Puchalt (University of Glasgow, UK) for sending strain RN450, Dr. C. Wolz (University of Tübingen, Germany) for sending

strains Newman, Newman-86 and Newman-86-199, and A. Toledo-Arana (Instituto de Agrobiotecnología, CSIC-Universidad Pública de Navarra, Spain) for strain ISP479r. Also special thanks to three anonymous reviewers for their helpful comments and suggestions. This study was funded by grants PCIN-2017-001 (AEI/FEDER, UE), Proyecto Intramural CSIC 201770E016, and IDI/2018/000119 (Asturias Innovation 2018-2020, Principado de Asturias, Spain and FEDER/EU).

Compliance with ethical standards

Conflict of interest The authors declare that they have no conflict of interest.

Publisher's note Springer Nature remains neutral with regard to jurisdictional claims in published maps and institutional affiliations.

References

- Erez Z, Steinberger-Levy I, Shamir M, Doron S, Stokar-Avihail A, Peleg Y, et al. Communication between viruses guides lysis-lysogeny decisions. *Nature*. 2017;541:488–93.
- Buckling A, Rainey PB. Antagonistic coevolution between a bacterium and a bacteriophage. *Proc Biol Sci*. 2002;269:931–6.
- Betts A, Kaltz O, Hochberg ME. Contrasted coevolutionary dynamics between a bacterial pathogen and its bacteriophages. *Proc Natl Acad Sci USA*. 2014;111:11109–14.
- Hall AR, Scanlan PD, Morgan AD, Buckling A. Host-parasite coevolutionary arms races give way to fluctuating selection. *Ecol Lett*. 2011;14:635–42.
- Gómez P, Ashby B, Buckling A. Population mixing promotes arms race host–parasite coevolution. *Proc R Soc*. 2015; B282:20142297.
- Vos M, Birkett PJ, Birch E, Griffiths RI, Buckling A. Local adaptation of bacteriophages to their bacterial hosts in soil. *Science*. 2009;325:833.

7. Heilmann S, Sneppen K, Krishna S. Sustainability of virulence in a phage-bacterial ecosystem. *J Virol.* 2010;84:3016–22.
8. Heilmann S, Sneppen K, Krishna S. Coexistence of phage and bacteria on the boundary of self-organized refuges. *Proc Natl Acad Sci USA.* 2012;109:12828–33.
9. Lourenço M, Chaffringeon L, Lamy-Besnier Q, et al. The spatial heterogeneity of the gut limits predation and fosters coexistence of bacteria and bacteriophages. *Cell Host Microbe.* 2020;28:1–12.
10. Bull JJ, Vegge CS, Schmerer M, Chaudhry WN, Levin BR. Phenotypic resistance and the dynamics of bacterial escape from phage control. *PLoS ONE.* 2014;9:e94690.
11. Chapman-McQuiston E, Wu XL. Stochastic receptor expression allows sensitive bacteria to evade phage attack. Part I: *Exp Biophys J.* 2008;94:4525–36.
12. Hadas H, Einav M, Fishov I, Zaritsky A. Bacteriophage T4 development depends on the physiology of its host *Escherichia coli*. *Microbiology.* 1997;143:179–85.
13. Abedon ST, Herschler TD, Stopar D. Bacteriophage latent-period evolution as a response to resource availability. *Appl Environ Microbiol.* 2001;67:4233–41.
14. Hoque MM, Naser IB, Bari SM, Zhu J, Mekalanos JJ, Faruque SM. Quorum regulated resistance of *Vibrio cholerae* against environmental bacteriophages. *Sci Rep.* 2016;6:37956.
15. Fernández L, Rodríguez A, García P. Phage or foe: an insight into the impact of viral predation on microbial communities. *ISME J.* 2018;12:1171–9.
16. Gödeke J, Paul K, Lassak J, Thormann KM. Phage-induced lysis enhances biofilm formation in *Shewanella oneidensis* MR-1. *ISME J.* 2011;5:613–26.
17. Rossmann FS, Racek T, Wobser D, Puchalka J, Rabener EM, Reiger M, et al. Phage-mediated dispersal of biofilm and distribution of bacterial virulence genes is induced by quorum sensing. *PLoS Pathog.* 2015;11:e1004653.
18. Liu X, Li Y, Guo Y, Zeng Z, Li B, Wood TK, et al. Physiological function of *rac* prophage during biofilm formation and regulation of *rac* excision in *Escherichia coli* K-12. *Sci Rep.* 2015;5:16074.
19. Rice SA, Tan CH, Mikkelsen PJ, Kung V, Woo J, Tay M, et al. The biofilm life cycle and virulence of *Pseudomonas aeruginosa* are dependent on a filamentous prophage. *ISME J.* 2009;3:271–82.
20. Hosseini Z, Tufenkji N, van de Ven TG. Formation of biofilms under phage predation: considerations concerning a biofilm increase. *Biofouling.* 2013;29:457–68.
21. Tan D, Dahl A, Middelboe M. Vibriophages differentially influence biofilm formation by *Vibrio anguillarum* strains. *Appl Environ Microbiol.* 2015;81:4489–97.
22. Fernández L, González S, Campelo AB, Martínez B, Rodríguez A, García P. Low-level predation by lytic phage phiIPLA-RODI promotes biofilm formation and triggers the stringent response in *Staphylococcus aureus*. *Sci Rep.* 2017;7:40965.
23. Dalebroux ZD, Svensson SL, Gaynor EC, Swanson MS. ppGpp conjures bacterial virulence. *Microbiol Mol Biol Rev.* 2010;74:171–99.
24. Nguyen D, Joshi-Datar A, Lepine F, Bauerle E, Olakanmi O, Beer K, et al. Active starvation responses mediate antibiotic tolerance in biofilms and nutrient-limited bacteria. *Science.* 2011;334:982–6.
25. Ochi K, Kandala JC, Freese E. Initiation of *Bacillus subtilis* sporulation by the stringent response to partial amino acid deprivation. *J Biol Chem.* 1981;256:6866–75.
26. He H, Cooper JN, Mishra A, Raskin DM. Stringent response regulation of biofilm formation in *Vibrio cholerae*. *J Bacteriol.* 2012;194:2962–972.
27. Gutiérrez D, Vandenheuvel D, Martínez B, Rodríguez A, Lavigne R, García P. Two Phages, phiIPLA-RODI and phiIPLA-C1C, lyse mono- and dual-species staphylococcal biofilms. *Appl Environ Microbiol.* 2015;81:3336–48.
28. Adams MH. Enumeration of bacteriophage particles. *Bacteriophages.* London: Interscience Publishers, Ltd; 1959. p. 27–34.
29. González S, Fernández L, Campelo AB, Gutiérrez D, Martínez B, Rodríguez A, et al. The behavior of *Staphylococcus aureus* dual-species biofilms treated with bacteriophage phiIPLA-RODI depends on the accompanying microorganism. *Appl Environ Microbiol.* 2017;83:e02821–16.
30. Herrera JJ, Cabo ML, Gonzalez A, Pazos I, Pastoriza L. Adhesion and detachment kinetics of several strains of *Staphylococcus aureus* subsp. *aureus* under three different experimental conditions. *Food Microbiol.* 2007;24:585–91.
31. Bryan D, El-Shibiny A, Hobbs Z, Porter J, Kutter EM. Bacteriophage T4 infection of stationary phase *Escherichia coli*: life after log from a phage perspective. *Front Microbiol.* 2016;7:1391.
32. González-Menéndez E, Fernández L, Gutiérrez D, Pando D, Martínez B, Rodríguez A, et al. Strategies to encapsulate the *Staphylococcus aureus* bacteriophage phiIPLA-RODI. *Viruses.* 2018;10:E495.
33. Sharp DG, Hock A, Taylor AE, Beard D, Beard JW. Sedimentation characters and pH stability of the T2 bacteriophage of *Escherichia coli*. *J Biol Chem.* 1946;165:259–70.
34. Langlet J, Gaboriaud F, Gantzer C. Effects of pH on plaque forming unit counts and aggregation of MS2 bacteriophage. *J Appl Microbiol.* 2007;103:1632–8.
35. Foulston L, Elsholz AK, DeFrancesco AS, Losick R. The extracellular matrix of *Staphylococcus aureus* biofilms comprises cytoplasmic proteins that associate with the cell surface in response to decreasing pH. *mBio.* 2014;5:e01667–14.
36. Dengler V, Foulston L, DeFrancesco AS, Losick R. An electrostatic net model for the role of extracellular DNA in biofilm formation by *Staphylococcus aureus*. *J Bacteriol.* 2015;197:3779–87.
37. Geiger T, Goerke C, Fritz M, Schäfer T, Ohlsen K, Liebeke M, et al. Role of the (p)ppGpp synthase RSH, a RelA/SpoT homolog, in stringent response and virulence of *Staphylococcus aureus*. *Infect Immun.* 2010;78:1873–83.
38. Azriel S, Goren A, Rahav G, Gal-Mor O. The stringent response regulator DksA is required for *Salmonella enterica* serovar Typhimurium growth in minimal medium, motility, biofilm formation, and intestinal colonization. *Infect Immun.* 2015;84:375–84.
39. Chuang YM, Dutta NK, Hung CF, Wu TC, Rubin H, Karakousis PC. Stringent response factors PPX1 and PPK2 play an important role in *Mycobacterium tuberculosis* metabolism, biofilm formation, and sensitivity to isoniazid in vivo. *Antimicrob Agents Chemother.* 2016;60:6460–70.
40. Díaz-Salazar C, Calero P, Espinosa-Portero R, Jiménez-Fernández A, Wirebrand L, Velasco-Domínguez MG, et al. The stringent response promotes biofilm dispersal in *Pseudomonas putida*. *Sci Rep.* 2017;7:18055.
41. Heilmann C, Hussain M, Peters G, Götz F. Evidence for autolysin-mediated primary attachment of *Staphylococcus epidermidis* to a polystyrene surface. *Mol Microbiol.* 1997;24:1013–24.
42. Liu Q, Wang X, Qin J, Cheng S, Yeo WS, He L, et al. The ATP-dependent protease ClpP inhibits biofilm formation by regulating Agr and cell wall hydrolase Sle1 in *Staphylococcus aureus*. *Front Cell Infect Microbiol.* 2017;7:181.
43. Gutiérrez D, Delgado S, Vázquez-Sánchez D, Martínez B, Cabo ML, Rodríguez A, et al. Incidence of *Staphylococcus aureus* and analysis of associated bacterial communities on food industry surfaces. *Appl Environ Microbiol.* 2012;78:8547–54.
44. Novick R. Properties of a cryptic high-frequency transducing phage in *Staphylococcus aureus*. *Virology.* 1967;33:155–66.
45. Toledo-Arana A, Merino N, Vergara-Irigaray M, Debarbouille M, Penades JR, Lasa I. *Staphylococcus aureus* develops an

- alternative, *ica*-independent biofilm in the absence of the *arlRS* two-component system. *J Bacteriol.* 2005;187:5318–29.
46. Duthie ES, Lorenz LL. Staphylococcal coagulase: mode of action and antigenicity. *J Gen Microbiol.* 1952;6:95–107.
47. Geiger T, Francois P, Liebeke M, Fraunholz M, Goerke C, Krismer B, et al. The stringent response of *Staphylococcus aureus* and its impact on survival after phagocytosis through the induction of intracellular PSMs expression. *PLoS Pathog.* 2012;8:e1003016.